SUPPORTING INFORMATION

CONTENTS

GENERAL INFORMATION

Instrumentation and Methods. ^{1}H NMR and ^{13}C NMR spectra were obtained on a 500 MHz Bruker BioDRX NMR spectrometer at the University of Pennsylvania NMR facility and were recorded at room temperature in deuterated acetonitrile (CD_3CN) or methanol (CD_3OD). Column chromatography was performed using silica gel (60 Å pore size, 40-75 μm particle size) from Sorbent Technologies. High-resolution mass spectrometry (HRMS) data were obtained using electrospray ionization (ESI) mass spectrometry on a Micromass Autospec at the Mass Spectrometry Center in the Chemistry Department at the University of Pennsylvania. Standard workup procedures involved multiple (~3) extractions with the indicated organic solvent, followed by washing of the combined organic extracts with water or brine, drying over sodium sulfate and removal of solvents *in vacuo*. All yields are reported after purification. ITC experiments were performed with GE Healthcare MicroCal™ iTC200 system. HP ^{129}Xe was generated using spin-exchange optical pumping (SEOP) method with a home-built ^{129}Xe hyperpolarizer, based on the commercial model IGI.Xe.2000 by GE. A gas mixture of 10% nitrogen, 89% helium, and 1% natural abundance xenon (Linde Group, NJ) was used as the hyperpolarizer input. 795 nm circularly polarized diode laser (OptiGrate SEOP Laser, 30 to 70 W) was used for optical pumping of Rb vapor. HP ^{129}Xe NMR measurements were performed on a Bruker BioDRX 500 MHz NMR spectrometer (138.12 MHz frequency for ^{129}Xe), using a 10-mm BBO NMR probe. Sample temperature was controlled by VT unit on NMR spectrometer to 300 ± 1 K. Chemical shifts were referenced relative to ^{129}Xe gas at 0 ppm when extrapolated to 0 atm.

Materials. All phosphate-buffered saline (PBS) used in this work was 1.058 mM potassium phosphate monobasic, 154 mM sodium chloride, and 5.6 mM sodium phosphate dibasic, pH 7.2. Avidin (10 mg, lyophilized) was purchased from Thermo Fisher Pierce. Organic reagents and solvents were used as purchased from the following commercial sources: *Sigma-Aldrich*: 1-butylamine (99.5%), triethylamine

(99.5%), cesium hydroxide monohydrate ($CsOH \cdot H_2O$, 95+%), 1-bromobutane (99%), 4-aminomethylbenzenesulfonamide (95%), 4-(2-aminoethyl)-benzenesulfonamide (99%); *Fisher*: pentylamine-biotin, hydrochloric acid, sodium sulfate (anhydrous), sodium chloride, sea sand (washed), potassium carbonate (K_2CO_3, anhydrous), ethyl acetate (EtOAc, HPLC grade), dichloromethane (CH_2Cl_2, HPLC grade), methanol (MeOH, HPLC grade), 1-butanol, 4 Å molecular sieves (Type 4A, 8-12 mesh beads); *Acros Organics*: N,N-dimethylformamide (DMF, anhydrous), acetonitrile (CH_3CN, anhydrous), deuterium oxide (D_2O), acetonitrile-*d*3 (CD_3CN); *Strem Chemicals*: cucurbit[6]uril monohydrate (CB[6], 99+%); *Alfa Aesar: p*-nitrophenyl acetate (98+%).

HYPER-CEST EXPERIMENTS

Prior to applying saturation pulse, a controllable amount of hp ^{129}Xe was delivered into a 3 mL sample solution and sealed in the NMR tube by a home-built continuous-flow gas delivery setup. For each data point in the Hyper-CEST spectrum, the gas mixture was bubbled for 20 s, followed by a 3-s delay to allow bubbles to collapse. Xe (all isotopes) concentration in Hyper-CEST experiments was ~136 μM = 4 mM/atm * 3.4 atm * 0.01 (Xe percentage in gas mixture). All Hyper-CEST experiments were carried out using a Bruker 500 MHz NMR spectrometer, with 10-mm PABBO probe. A 90° hard pulse of this probe has pulse length of 22 μs. For Hyper-CEST frequency-scan profile (Figures 3 and 4), Dsnob saturation pulse with 690 Hz bandwidth was used. Pulse length t_{pulse} = 3.80 ms, field strength $B_{1,max}$ = 77 μT, number of pulses n_{pulse}= 400, saturation time t_{sat} = 1.52 s. For Figure 5, Dsnob saturation pulse with 276 Hz bandwidth was used. Pulse length t_{pulse} = 9.50 ms, field strength $B_{1,max}$ = 30.8 μT, number of pulses n_{pulse}= 400, saturation time t_{sat} = 3.80 s.

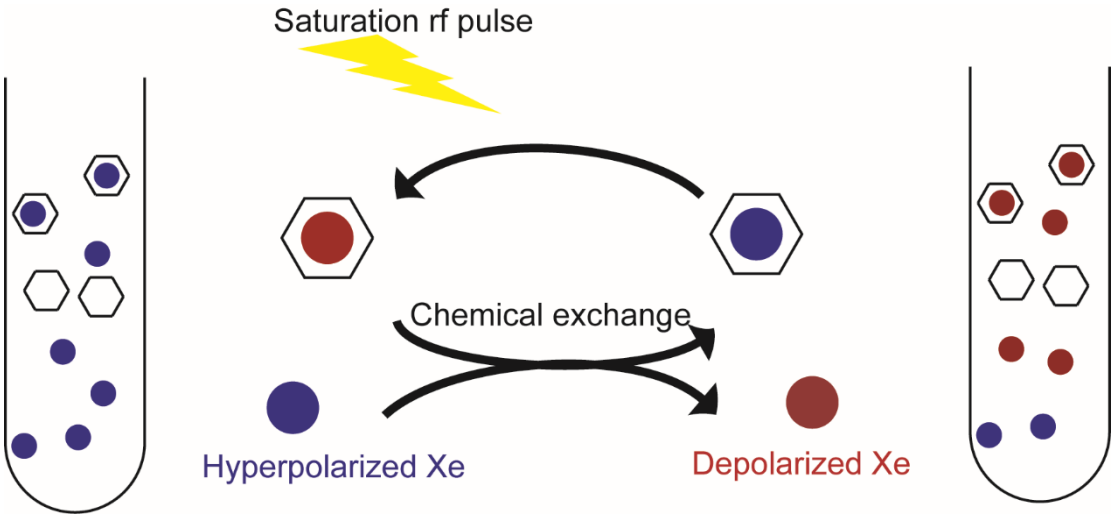

Scheme S1: Hyper-CEST NMR mechanism. Xenon-binding CB[6] molecules are represented by hexagons.

SYNTHETIC PROCEDURES FOR TFGS

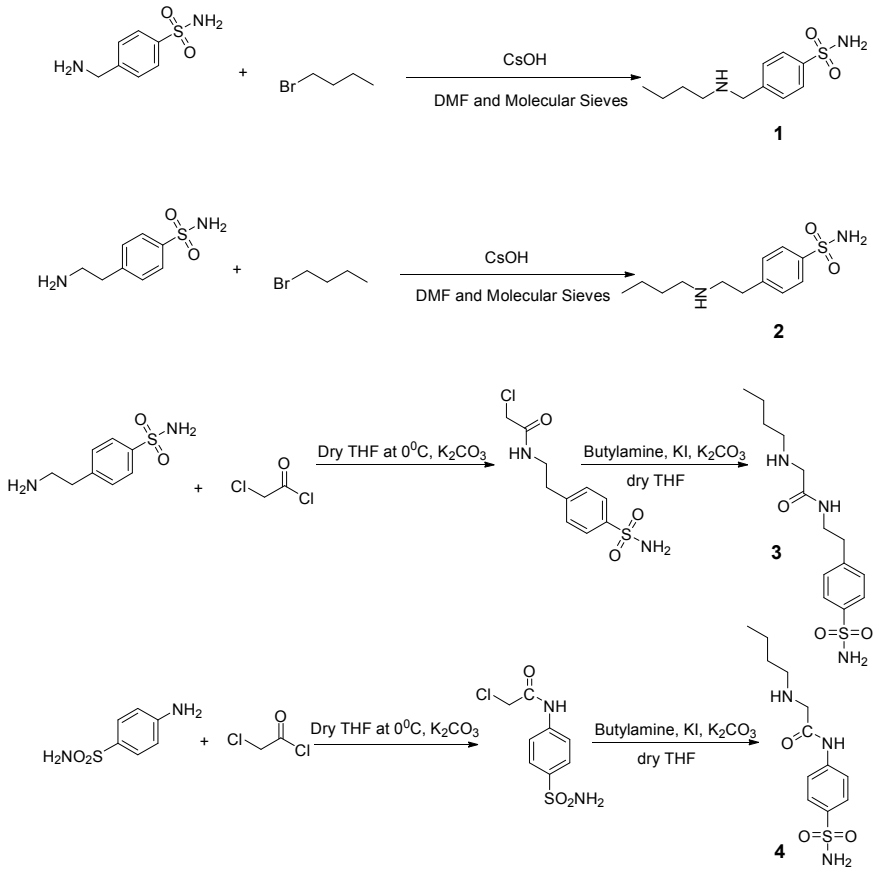

Scheme S2: Synthetic methods for TFGs

Synthesis of 1, 2.[1]

4-[(butylamino)methyl]-benzenesulfonamide (***1***) *and 4-[2-(butylamino)ethyl]benzenesulfonamide* (***2***) were synthesized in one step with yields of 30% and 43%. Taking **2** as an example, in an oven-dried flask with a suspension containing 4 Å molecular sieves (500 mg) and anhydrous DMF (8.3 mL), cesium hydroxide monohydrate (285.5 mg, 1.7 mmol, 1 equiv) was added. The mixture was stirred vigorously for 10 min. Then, 4-(2-aminoethyl)benzenesulfonamide (340.4 mg, 1.7 mmol, 1 equiv) was added to the flask and the reaction mixture was stirred vigorously for 30 min. 1-bromobutane (0.1826 mL, 1.7 mmol, 1 equiv) was added to the white suspension and the reaction proceeded for 20 h at rt. Then the reaction mixture was filtered and washed several times with ethyl acetate. The filtrate was concentrated and taken up in 1 M NaOH. Ethyl acetate (5 x 20 mL) was used to extract the product and standard workup

procedures followed. The crude mixture was purified by column chromatography using a gradient of ethyl acetate to 5% methanol in ethyl acetate (v/v). The purified 4-[2-(butylamino)ethyl]benzenesulfonamide (***2***) was a white powder.

^{1}H NMR δ(ppm) for **1** (500 MHz, methanol-d4) 7.90 (d, J = 8.4, 2H), 7.57 (d, J = 8.4, 2H), 3.99 (s, 2H), 2.75 (t, J = 7.6, 2H), 1.62-1.56 (m, 2H), 1.42-1.34 (m, 2H), 0.95 (t, J = 7.7, 3H). ^{13}C NMR ($CDCl_3$) δ(ppm): 144.7, 142.3, 130.6, 127.5, 53.0, 31.4, 24.1, 21.3, 14.2. HRMS (m/z): $[M+H]^+$ calcd. for $C_{11}H_{18}N_2O_2S$, 243.1167; found, 243.1165.

^{1}H NMR δ(ppm) for **2** (500 MHz, methanol-d4) 7.45(d, J = 8.3, 2H), 7.57 (d, J = 8.3, 2H), 3.15(t, J = 8.0, 2H), 3.04(t, J = 8.0, 2H), 2.92(t, J = 8.0, 2H), 1.67-1.61 (m, 2H), 1.45-1.38(m, 2H), 0.97 (t, J = 7.4, 3H). ^{13}C NMR ($CDCl_3$) δ(ppm): 143.8, 143.4, 130.4, 127.7, 50.0, 33.9, 30.1, 24.2, 21.0, 14.0. HRMS (m/z): $[M+H]^+$ calcd. for $C_{12}H_{20}N_2O_2S$, 257.1324; found, 257.1321.

Synthesis of 3, 4.

2-(butylamino)-N-(4-sulfamoylphenethyl)acetamide ***(3)*** and *2-(butylamino)-N-(4-sulfamoylphenyl)acetamide* ***(4)*** were synthesized through two step reactions. In the first step[2] *2-chloro-N-(4-sulfamoylphenyl)acetamide* or *2-chloro-N-(4-sulfamoylphenethyl)acetamide* was produced by reacting 4-aminobenzenesulfonamide or 4-(2-aminoethyl)-benzenesulfonamide with chloroacetyl chloride in ~70% yield. In a round bottom flask, 4-(2-aminoethyl)-benzenesulfonamide (1.2 g, 6.02 mmol, 1 equiv) and K_2CO_3 (1.66g, 12.04 mmol, 2 equiv) were dissolved in 30 mL anhydrous THF. Flask was allowed to cool for 10 min on ice with stirring under N_2 atmosphere. Chloroacetyl chloride (0.6 mL, 7.23 mmol, 1.2 equiv) was added dropwise under N_2 atmosphere and the mixture was stirred for another 30 min. Water (20 mL) was added to the mixture to quench the reaction, while stirring was continued for another 5 min. The organic layer was separated and the aqueous layer was extracted with EtOAc (100 mL x 3). The combined organic layer was washed with brine, dried over anhydrous Na_2SO_4, concentrated in *vacuo* and purified by recrystallization in hexane : MeOH.

In the second step[3] *2-chloro-N-(4-sulfamoylphenethyl)acetamide* (1.01 g, 3.65 mmol, 0.7 equiv) and butylamine (528 mg, 5.21 mmol, 1 equiv) were dissolved in anhydrous THF (35 mL) under N_2 with stirring. K_2CO_3 (2.15 g, 15.6 mmol, 3 equiv) and KI (433 mg, 2.61 mmol, 0.5 mmol) were then added to the mixture, and reflux was continued for 17 h. The reaction mixture was concentrated *in vacuo*, extracted with acetone (50 mL x 3), and centrifuged. The supernatant was concentrated and then purified with flash chromatography (SiO_2, $CHCl_3$/MeOH/NH_4OH 100:5:1) as a white solid (640 mg, 2.04 mmol, 56%).

^{1}H NMR δ(ppm) for **3** (500 MHz, methanol-d4) 7.85 (d, J = 8.9, 2H), 7.77 (d, J = 8.9, 2H), 3.41 (s, 2H), 2.63 (t, J = 7.2, 2H), 1.56-1.50 (m, 2H), 1.44-1.36(m, 2H), 0.95 (t, J = 7.3, 3H). ^{13}C NMR ($CDCl_3$) δ(ppm): 174.3, 145.3, 143.2, 130.4, 127.4, 52.8, 41.2, 36.4, 32.8, 25.4, 21.5, 14.3. HRMS (m/z): $[M+H]^+$ calcd. for $C_{14}H_{23}N_3O_3S$, 314.1538; found, 314.1524.

^{1}H NMR δ(ppm) for **4** (500 MHz, Acetonitrile-d3) 7.78 (d, J = 8.4, 2H), 7.40 (d, J = 8.4, 2H), 3.49-3.43(m, 2H), 3.06 (s, 2H), 2.87 (t, J = 7.0, 2H), 2.44 (t, J = 7.0, 2H), 1.41-1.24(m, 4H), 0.89 (t, J = 7.2, 3H). ^{13}C NMR ($CDCl_3$) δ(ppm): 172.5, 143.2, 139.9, 128.3, 120.5, 53.4, 50.3, 32.8, 21.5, 14.3. HRMS (m/z): $[M+H]^+$ calcd. for $C_{12}H_{19}N_3O_3S$, 286.1225; found, 286.1230.

PROTEIN EXPRESSION AND PURIFICATION

A previously-prepared[4] ampicillin-resistant pCAM plasmid containing the full-length human CAII gene (GenBank accession no. AAA51909) was transformed into *E. coli* BL21(DE3) competent cells. Cells were grown in 6 L of LB media supplemented with 100 μg/mL ampicillin at 250 rpm and 37 °C to an optical density of ~0.6 at 600 nm. Protein expression was induced by adding 1 mM isopropyl-β-D-thiogalactopyranoside and 1 mM $ZnSO_4$ (final concentrations). The cells were incubated overnight at 250 rpm and 18 °C. The cells were pelleted by centrifugation and frozen at -80 °C for long-term storage.

The frozen cell pellet was thawed and resuspended in lysis buffer [50 mM sodium phosphate (pH 7.4), 0.3 M NaCl]. The cells were lysed by two additional rounds of freezing and thawing. The lysate was clarified by centrifugation, and the supernatant was loaded onto a 5 mL HisTrap HP nickel immobilized-metal affinity chromatography column (GE Healthcare Life Sciences) in 50 mM sodium phosphate (pH 7.4), 0.3 M NaCl. CAII was eluted with 50 mM sodium phosphate (pH 7.4), 0.3 M NaCl, 0.5 M imidazole. Fractions containing CAII were pooled, concentrated with an Amicon Ultra-15 centrifugal filter (MWCO = 10 kDa), and further purified by size exclusion chromatography in 50 mM Tris (pH 8.0), 10% glycerol using a HiLoad 26/60 Superdex column (GE Healthcare Life Sciences). Fractions containing CAII were pooled and concentrated to 45 mg/mL. Analysis by SDS-PAGE indicated that the protein was over 95% pure. CAII concentration was determined by measuring absorbance at 280 nm (ε_{280} = 57 000 M^{-1} cm^{-1}).

CRYSTALLIZATION

Materials and methods

CAII crystals were grown by the hanging drop vapor diffusion method. 4.0 μL of protein solution [44 mg/mL CAII in 50 mM Tris (pH 8.0), 10% glycerol] was mixed with 4.0 μL of precipitant solution [50 mM Tris (pH 7.0), 1.3 M sodium citrate] on a siliconized glass cover slide (Hampton Research). The hanging drop was suspended over a 1.0 mL reservoir of precipitant solution. The hanging drops remained clear after three weeks of incubation at 4 °C. To facilitate crystallization, the crystallization tray was moved to a 21 °C incubator and the hanging drops were microseeded by a seeding tool (Hampton Research) with CAII crystals previously grown in the same condition. Thick rectangular crystals appeared over the course of several weeks.

CAII crystals were soaked with two-faced guest (TFG) ligands **1**, **3**, and **4** as follows: individual CAII crystals were transferred to a 10.0 μL drop of 50 mM Tris (pH 7.0), 1.3 M sodium citrate, 2.5% (v/v)

DMSO containing 1 mM ligand. The sitting drop was equilibrated against a 400 μL reservoir of 50 mM Tris (pH 7.0), 1.3 M sodium citrate. CAII crystals were soaked with ligand overnight at 21 °C. The crystals were transferred to cryoprotectant solution [soak solution supplemented with 30% (v/v) glycerol] and then flash-cooled in liquid nitrogen.

X-ray diffraction data from single crystals of CAII-**1** and CAII-**4** were collected at beamline 14-1 at the Stanford Synchrotron Radiation Lightsource (SSRL). X-ray diffraction data from single crystals of CAII-**3** were collected at beamline 24ID-E at the Advanced Photon Source (APS). Diffraction data were integrated using iMosflm (version 7.1.1)[5] and processed using AIMLESS[6] from the CCP4 suite of programs.[7] Each structure was solved by molecular replacement and refined in the PHENIX (version 1.9)[8] suite of programs. Initial phases for the CAII-**1** model were calculated from an isomorphous high-resolution CAII structure (PDB ID 3KS3)[9] less the solvent and ions, and initial phases for CAII-**3** and CAII-**4** models were calculated from the refined model of CAII-**1** less the ligand, solvent, and ions.

Structure refinement was performed in PHENIX and manual model adjustments were made in COOT (version 0.8.1).[10] Atomic coordinates for **1**, **3**, **4**, and glycerol were generated using ChemDraw (version 14.0) and Chem3D Pro (version 14.0), and geometric restraints were generated using eLBOW.[11] The B-factors of protein atoms, ligand atoms, and ions were refined anisotropically whereas the B-factors of solvent molecules were refined isotropically. Disordered protein atoms showing no electron density in the $2F_o$-F_c map were deleted from the protein model. Refinement proceeded until R_{free} converged at its lower limit. The quality of the final model was assessed using MolProbity.[12] Data collection and refinement statistics for all structure determinations are recorded in Table S1. Figures were generated using PyMOL,[13] and the surface representations were colored according to the hydrophobicity scale defined by Eisenberg *et. al*.[14]

TFG inhibitors **1**, **3**, and **4** bind the active site of CAII in typical fashion for arylsulfonamides: the sulfonamidate (N) coordinates to the catalytic Zn^{2+} and donates a hydrogen bond to the hydroxyl oxygen of T199, and a sulfonamide oxygen accepts a hydrogen bond from the backbone amide nitrogen of T199. The butyl tails of inhibitors **3** and **4** are both disordered, and, interestingly, whereas the inhibitor tail of **3** adopts only the *trans*-amide conformation, the inhibitor tail of **4** appears to adopt both *cis*- and *trans*-amide conformations. During refinement the *cis*- and *trans*-amide conformations of **4** converged to occupancies of 0.63 and 0.37, respectively.

Table S1. Data collection and refinement statistics

	CAII–**1** complex	CAII–**3** complex	CAII–**4** complex
Unit cell			
space group symmetry	$P2_1$	$P2_1$	$P2_1$
a, b, c (Å)	42.4, 41.4, 72.1	42.4, 41.4, 72.1	42.3, 41.4, 72.0
α, β, γ (°)	90.0, 104.0, 90.0	90.0, 104.2, 90.0	90.0, 104.1, 90.0
Data collection[a]			
wavelength (Å)	1.282	0.979	1.282
resolution limits (Å)	41.4-1.34	41.4-1.13	41.4-1.33
total/unique reflections	388992/51140	631318/87628	400949/52900
R_{merge}[b]	0.047 (0.235)	0.080 (0.372)	0.048 (0.198)
$I/\sigma(I)$	24.2 (7.8)	17.4 (7.4)	23.6 (8.9)
$CC_{1/2}$	0.999 (0.969)	0.996 (0.922)	0.999 (0.977)
multiplicity	7.6 (7.6)	7.2 (6.1)	7.6 (7.5)
completeness (%)	93.8 (88.6)	96.6 (92.8)	95.3 (91.7)
Refinement			
reflections used in refinement/test set	100221/5042	172159/8740	103676/5244
R_{work}[c]	0.137	0.134	0.142

R_{free} [d]	0.162	0.151	0.167
protein atoms	2038	2045	2029
water molecules	255	272	231
ligand molecules	1	1	1
Zn^{2+} ions	1	1	1
Na^{+} ions	1	1	1
glycerol molecules	1	1	1
R.m.s. deviations from ideal geometry			
bonds (Å)	0.005	0.005	0.006
angles (°)	1.1	1.2	1.2
dihedral angles (°)	12.8	12.7	13.7
Average B-factors (Å^2)			
Protein	11	9	11
Solvent	25	22	24
Ligand	15	15	13
Zn^{2+}	11	4	11
Ramachandran plot (%) [e]			
favored	96.9	96.5	97.3
allowed	3.1	3.5	2.7
outliers	0	0	0
PDB accession code	**5EKH**	**5EKJ**	**5EKM**

[a] Values in parentheses refer to the highest shell of data.
[b] $R_{merge} = \sum|I_h - \langle I\rangle_h|/\sum I_h$, where $\langle I\rangle_h$ is the average intensity for reflection h calculated from replicate reflections.
[c] $R_{work} = \sum||F_o| - |F_c||/\sum|F_o|$ for reflections contained in the working set. $|F_o|$ and $|F_c|$ are the observed and calculated structure factor amplitudes, respectively.
[d] $R_{free} = \sum||F_o| - |F_c||/\sum|F_o|$ for reflections contained in the test set held aside during refinement.
[e] Calculated with MolProbity.

FIGURES:

Figure S1. ITC Data

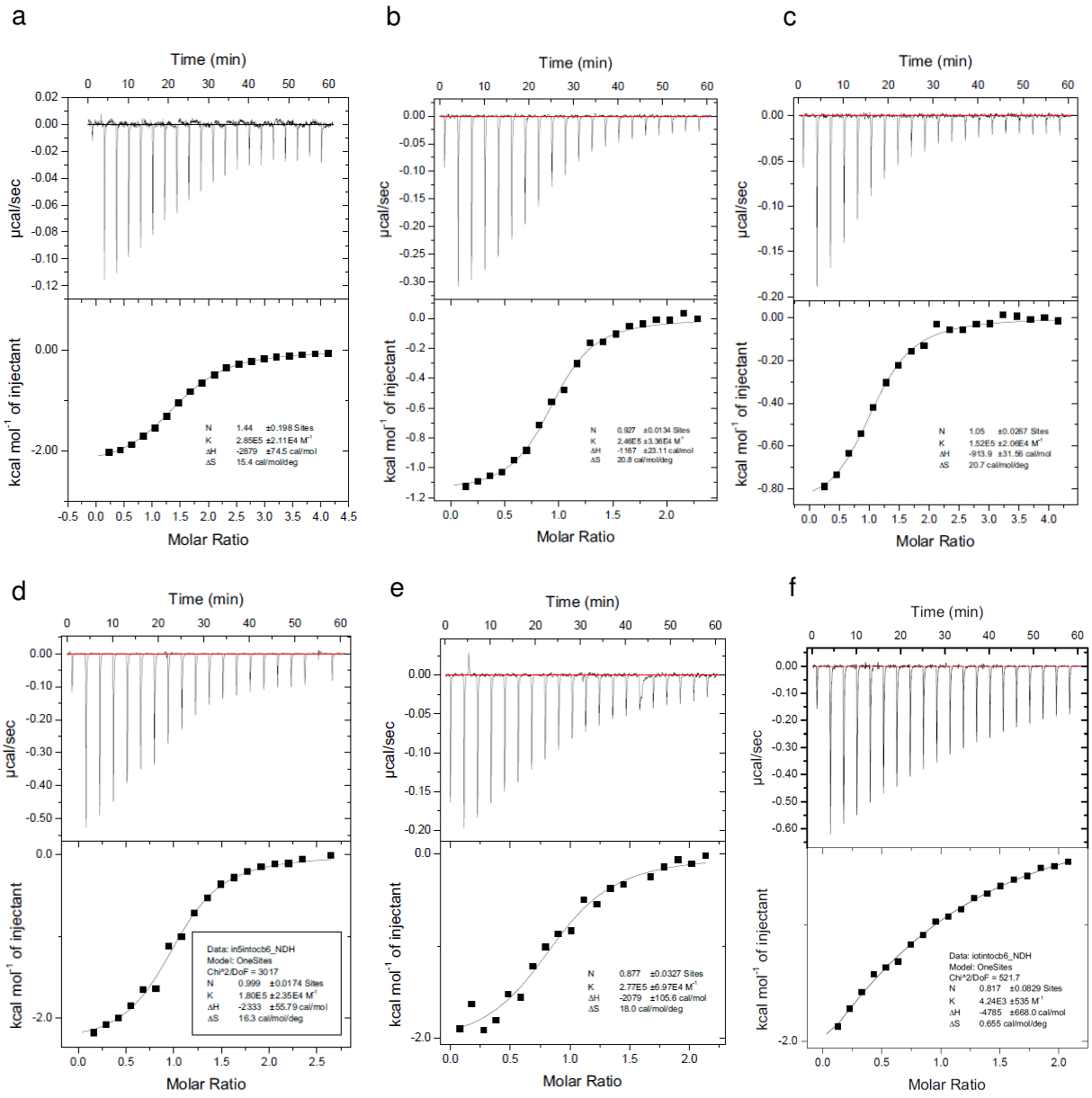

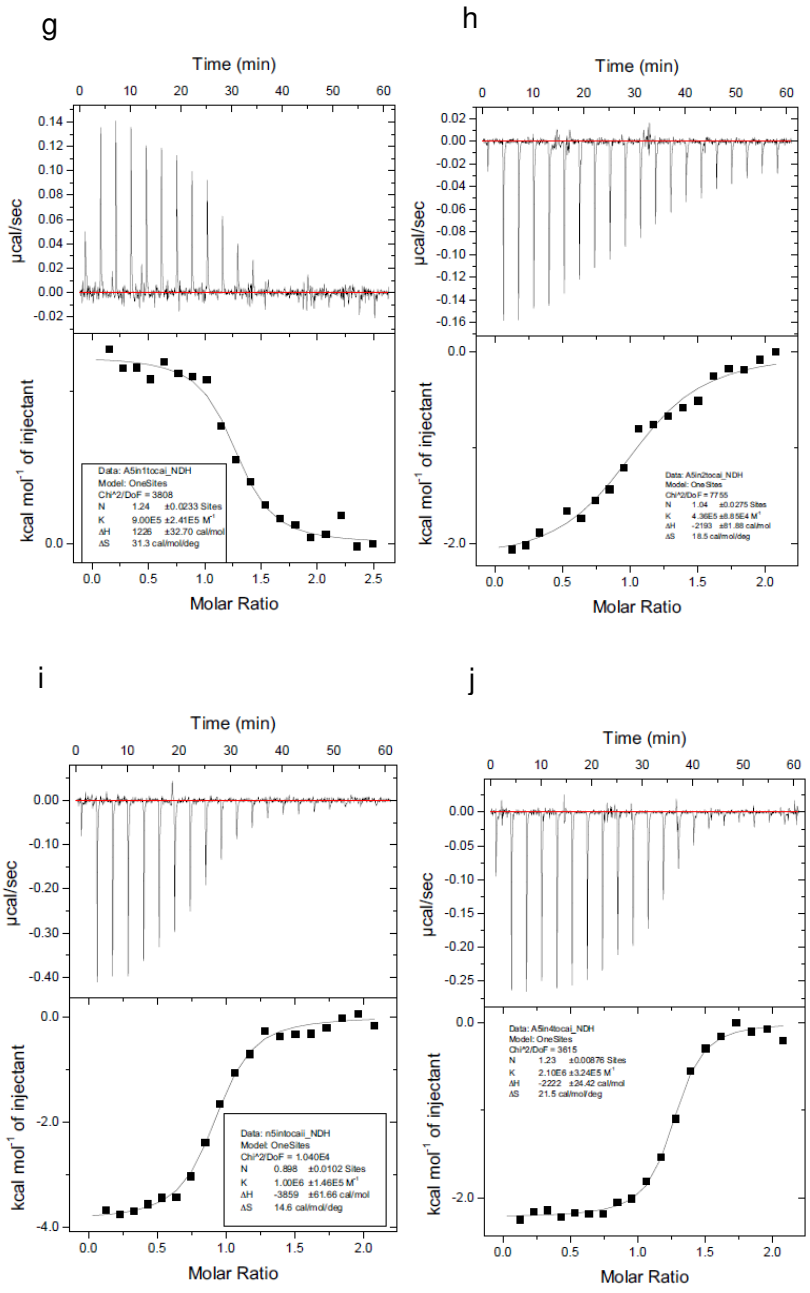

Figure S1. ITC data for butylamine binding to CB[6] (a), **1** to CB[6] (b), **2** to CB[6] (c), **3** to CB[6] (d), **4** to CB[6] (e), **5** to CB[6] (f), **1** to CAII (g), **2** to CAII (h), **3** to CAII (i), **4** to CAII (j).

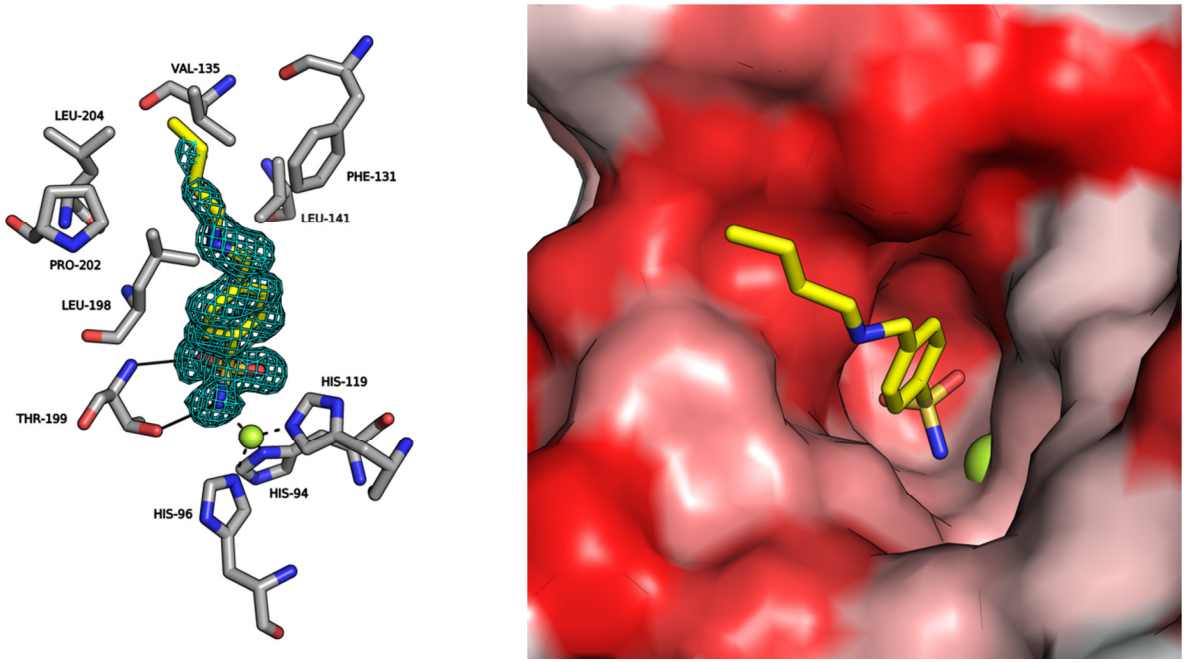

Figure S2. TFG 1 bound to CAII. (Left) simulated annealing omit map (contoured at 2.1σ) showing **1** bound in the active site of CAII. Coordination bonds are shown as dashed black lines and hydrogen bonds are shown as solid black lines. The active site Zn^{2+} is shown as a green sphere. (Right) The active site channel of CAII represented as a surface model (hydrophobic residues in red; hydrophilic residues in white).

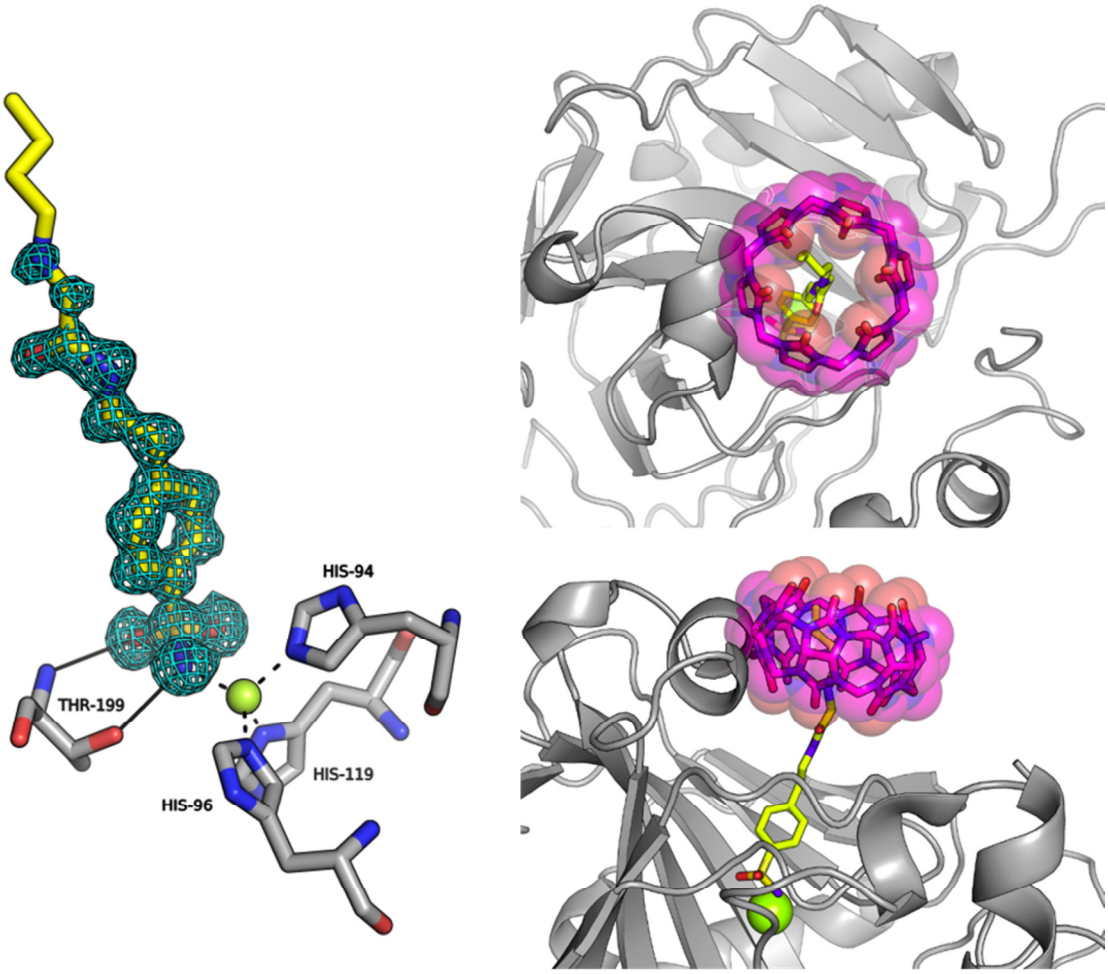

Figure S3. TFG 3 bound to CAII. (Left) simulated annealing omit map (contoured at 3σ) showing **3** bound in the active site of CAII. Coordination bonds are shown as dashed black lines and hydrogen bonds are shown as solid black lines. The active site Zn^{2+} is shown as a green sphere. (Right) Modeling CB[6] binding to the CAII-TFG**4** complex showing steric clash between CB[6] and CAII, top view and side view.

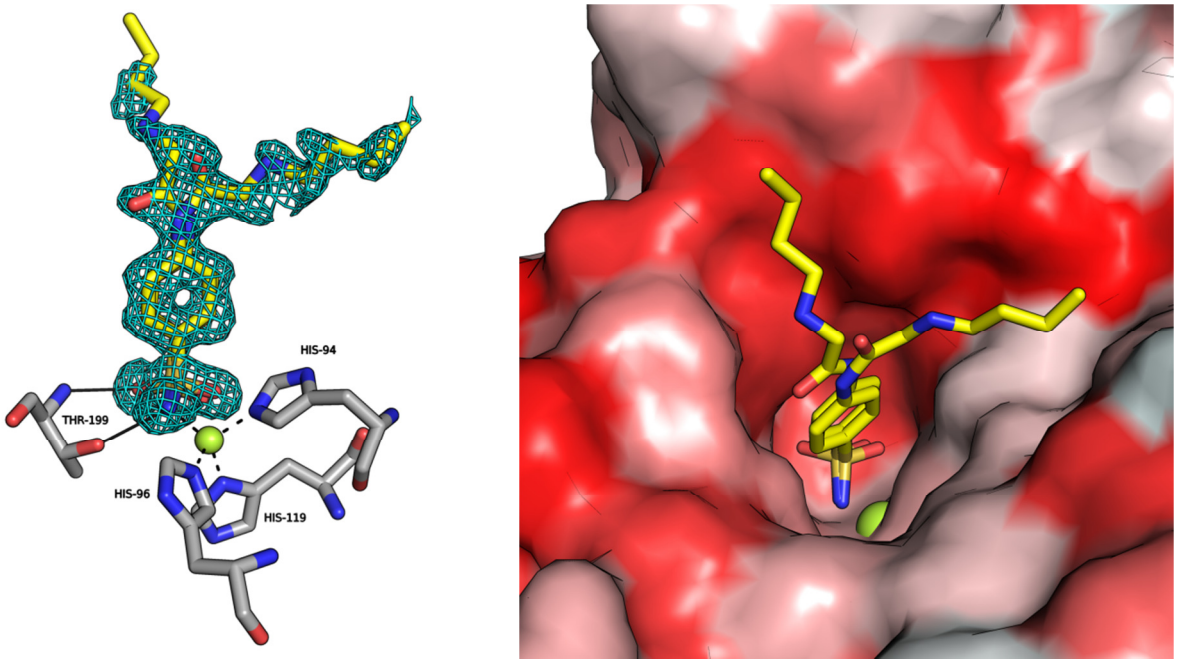

Figure S4. TFG 4 bound to CAII. (Left) simulated annealing omit map (contoured at 2.5σ) showing **4** bound in the active site of CAII. Coordination bonds are shown as dashed black lines and hydrogen bonds are shown as solid black lines. The active site Zn^{2+} is shown as a green sphere. (Right) The active site channel of CAII represented as a surface model (hydrophobic residues in red; hydrophilic residues in white).

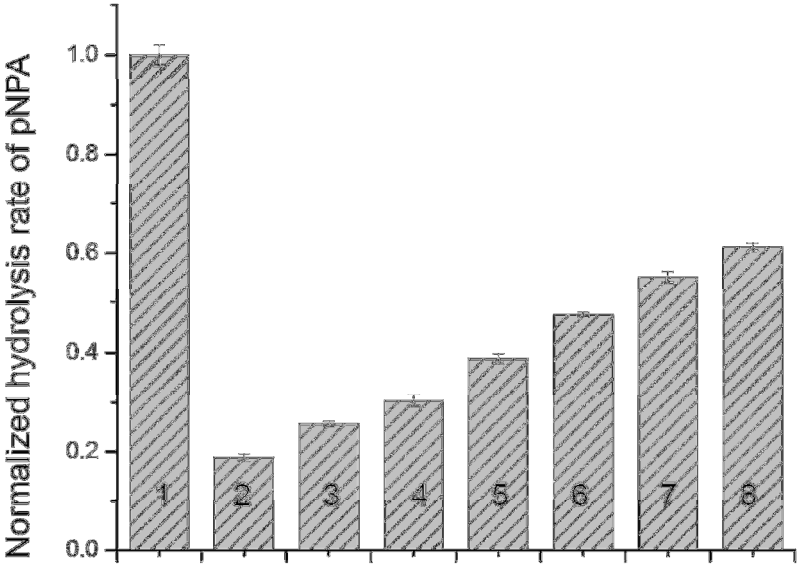

Figure S5. CAII esterase activity in the presence of different ratios of TFG 4 and CB[6]. Sample composition 1: 5μM CAII; 2: 5μM CAII + 10μM TFG **4**; 3: 5μM CAII + 10μM TFG **4** + 10μM CB[6]; 4: 5μM CAII + 10μM TFG **4** + 20μM CB[6]; 5: 5μM CAII + 10μM TFG **4** + 50μM CB[6]; 6: 5μM CAII + 10μM TFG **4** + 100μM CB[6]; 7: 5μM CAII + 10μM TFG **4** + 200μM CB[6]; 8: 5μM CAII + 10μM TFG **4** + 500μM CB[6]. Standard errors were determined from three or more replicates for each condition.

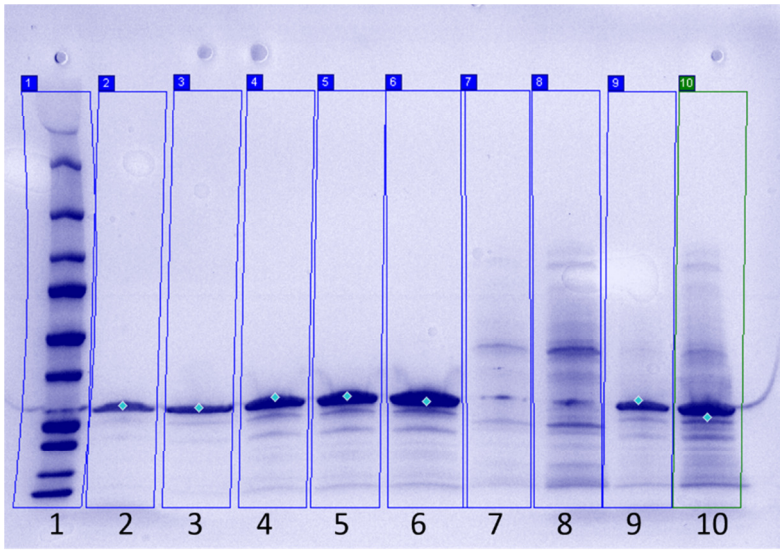

Figure S6. SDS-PAGE profile Lane 1: standard protein ladder; Lanes 2- 6 contain 0.6, 0.6, 0.9, 1.2, 2.0 µg of purified protein. Lanes 7 and 8 contain 20 µL control *E.coli* lysate with OD_{600nm} = 0.5 and 1. Lanes 9 and 10 contain 20 µL transformed and induced *E.coli* lysate with OD_{600nm} = 0.5 and 1. Analysis of band intensity showed that lane 9 contains 0.6 µg CAII and lane 10 contains 1.2 µg CAII (2.07 µM).

^{1}H NMR AND ^{13}C NMR SPECTRA OF COMPOUNDS SYNTHESIZED IN THIS STUDY

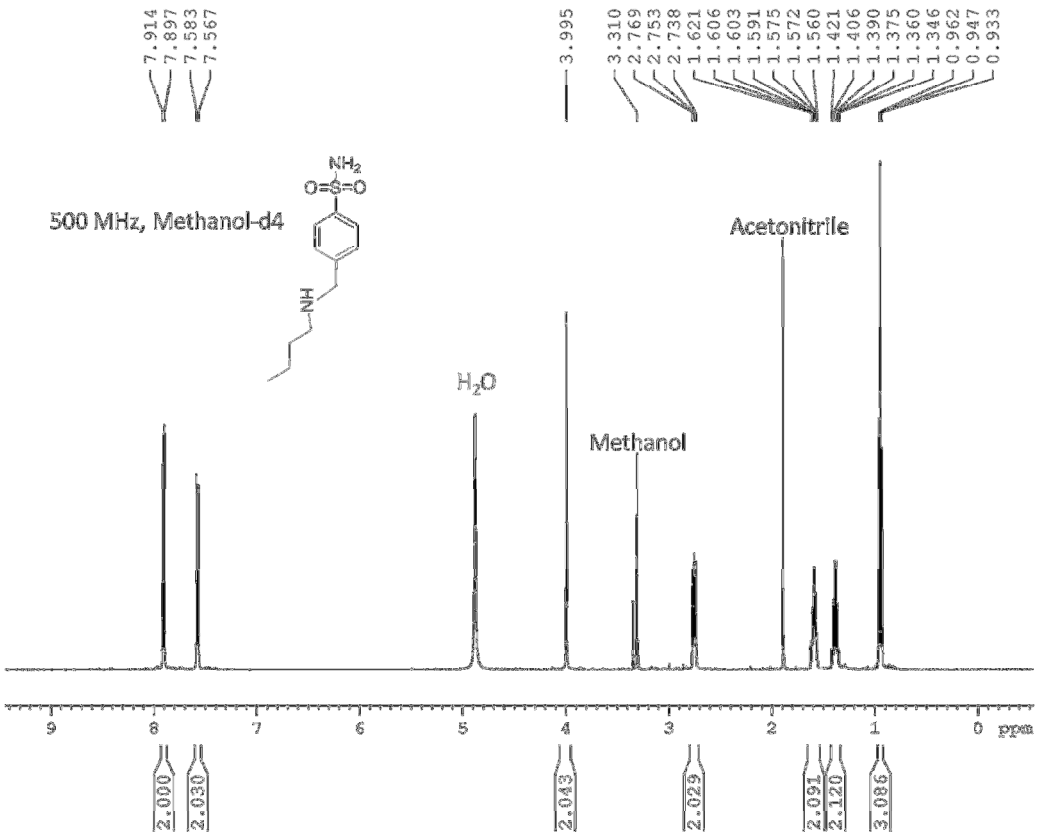

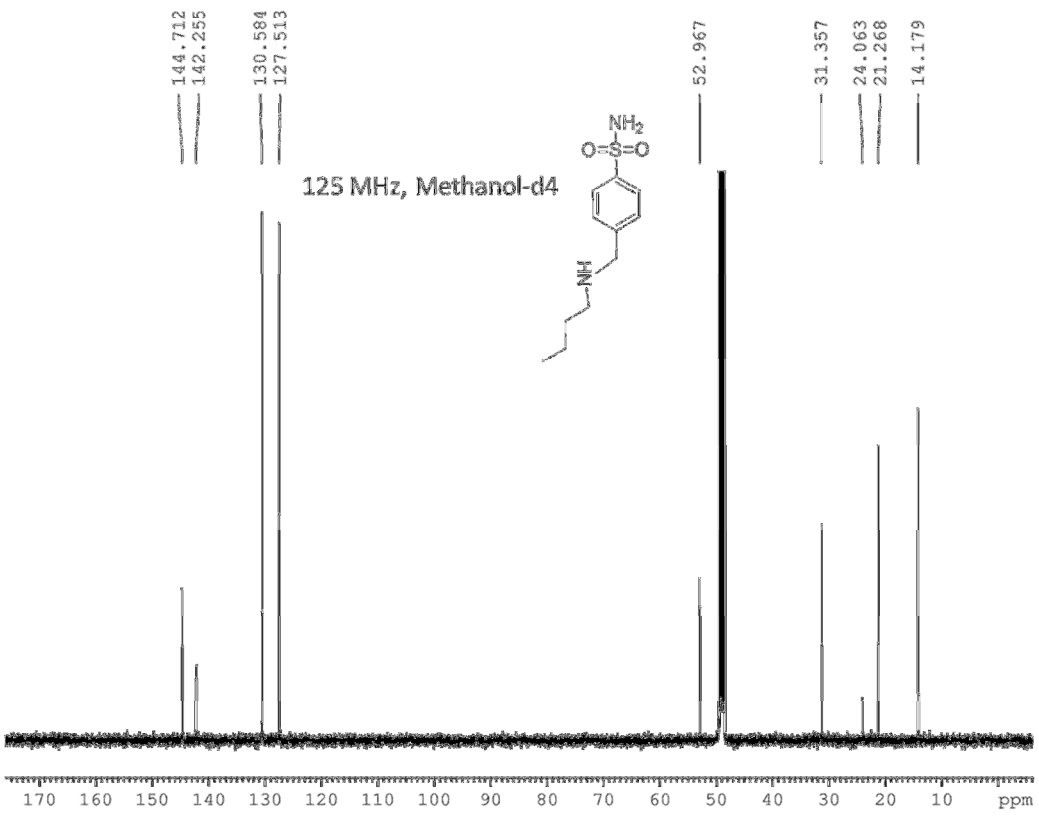
144.712
142.255
130.584
127.513
52.967
31.357
24.063
21.268
14.179
125 MHz, Methanol-d4
NH2
O=S=O
NH
170 160 150 140 130 120 110 100 90 80 70 60 50 40 30 20 10 ppm

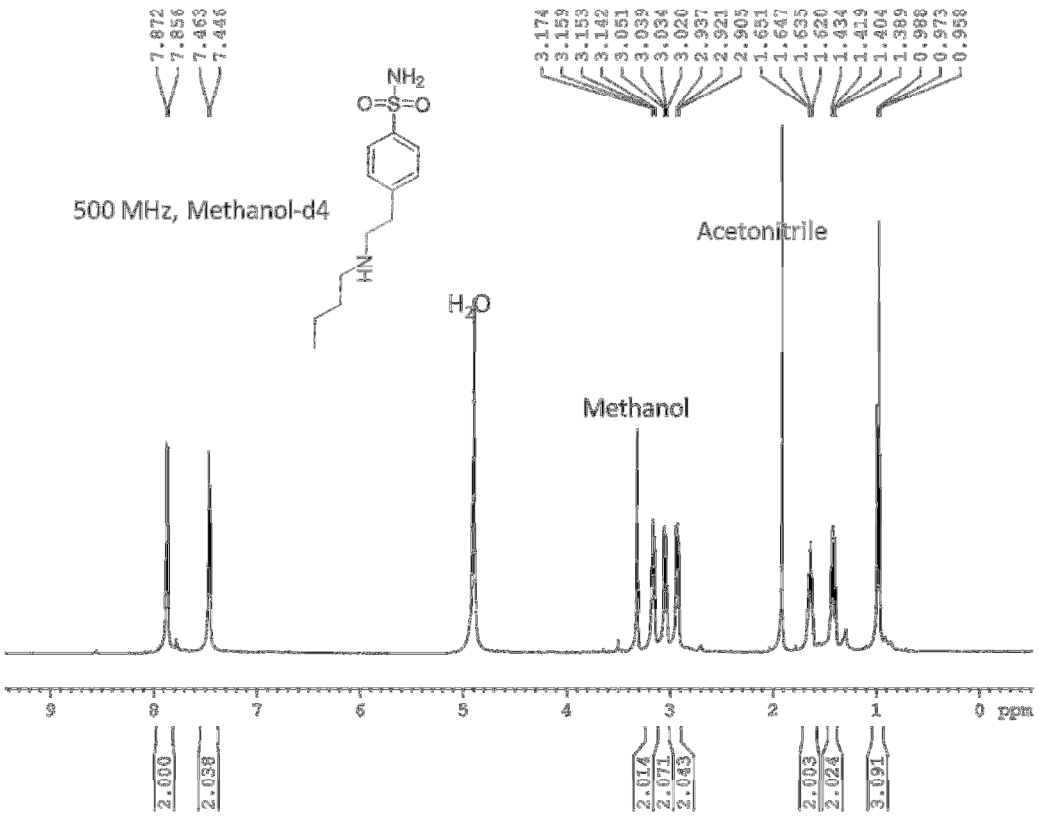
7.872
7.856
7.463
7.446
3.174
3.159
3.153
3.142
3.051
3.039
3.034
3.020
2.937
2.921
2.905
1.651
1.647
1.635
1.620
1.434
1.419
1.404
1.389
0.988
0.973
0.958
NH2
O=S=O
HN
500 MHz, Methanol-d4
H2O
Methanol
Acetonitrile
9
8
7
6
5
4
3
2
1
0 ppm
2.000
2.038
2.014
2.071
2.043
2.003
2.024
3.191

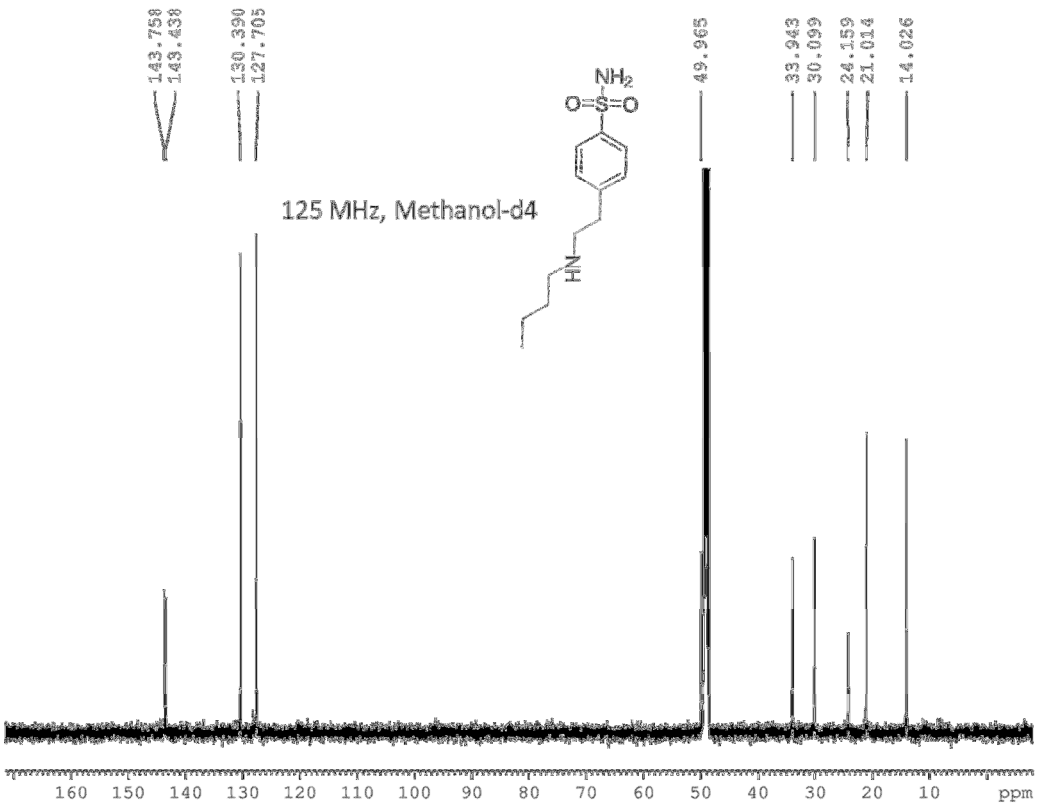
143.758
143.438
130.390
127.705
49.965
33.943
30.099
24.159
21.014
14.026
125 MHz, Methanol-d4
NH2
O=S=O
HN
160 150 140 130 120 110 100 90 80 70 60 50 40 30 20 10 ppm

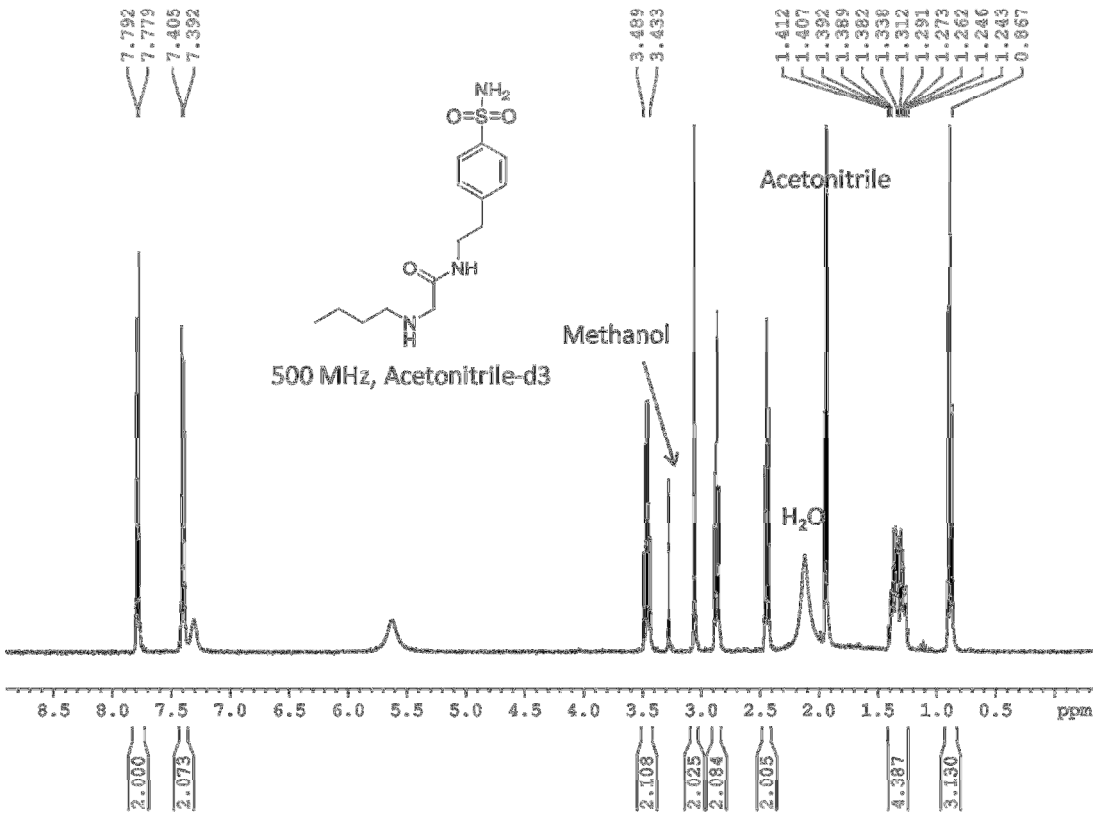
7.792
7.779
7.405
7.392
3.489
3.433
1.412
1.407
1.392
1.389
1.382
1.338
1.312
1.291
1.273
1.262
1.246
1.243
0.867
NH2
O=S=O
O
NH
N
H
Acetonitrile
Methanol
H2O
500 MHz, Acetonitrile-d3
8.5 8.0 7.5 7.0 6.5 6.0 5.5 5.0 4.5 4.0 3.5 3.0 2.5 2.0 1.5 1.0 0.5 ppm
2.000
2.073
2.108
2.025
2.084
2.005
4.387
3.130

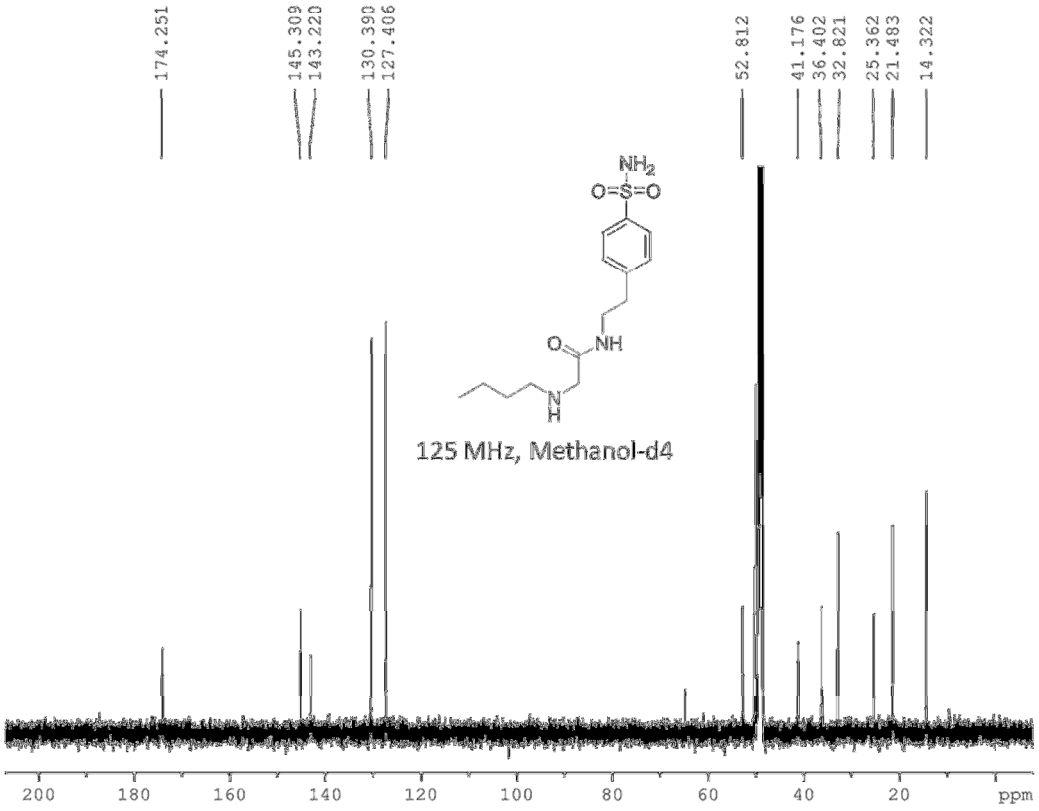
174.251
145.309
143.220
130.390
127.406
52.812
41.176
36.402
32.821
25.362
21.483
14.322
NH2
O=S=O
O
NH
N
H
125 MHz, Methanol-d4
200
180
160
140
120
100
80
60
40
20
ppm

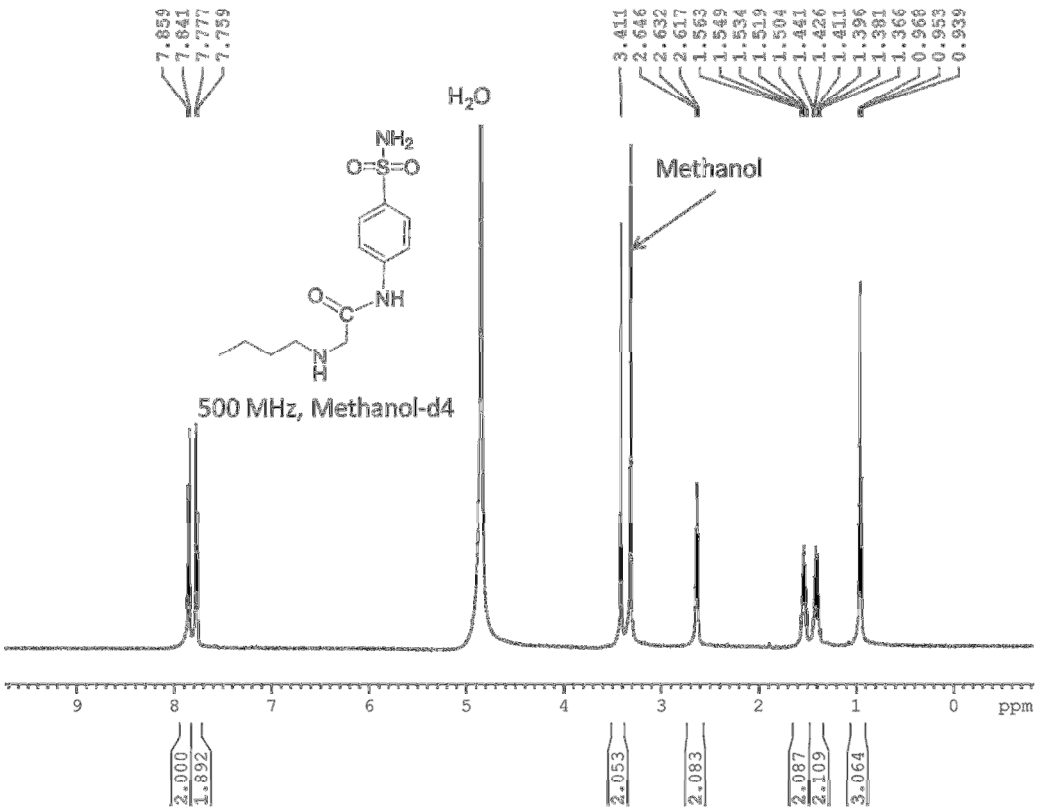
7.859
7.841
7.777
7.759
3.411
2.646
2.632
2.617
1.563
1.549
1.534
1.519
1.504
1.441
1.426
1.411
1.396
1.381
1.366
0.966
0.953
0.939
H2O
Methanol
NH2
O=S=O
O
C
NH
N
H
500 MHz, Methanol-d4
9
8
7
6
5
4
3
2
1
0
ppm
2.000
1.892
2.053
2.083
2.087
2.109
3.064

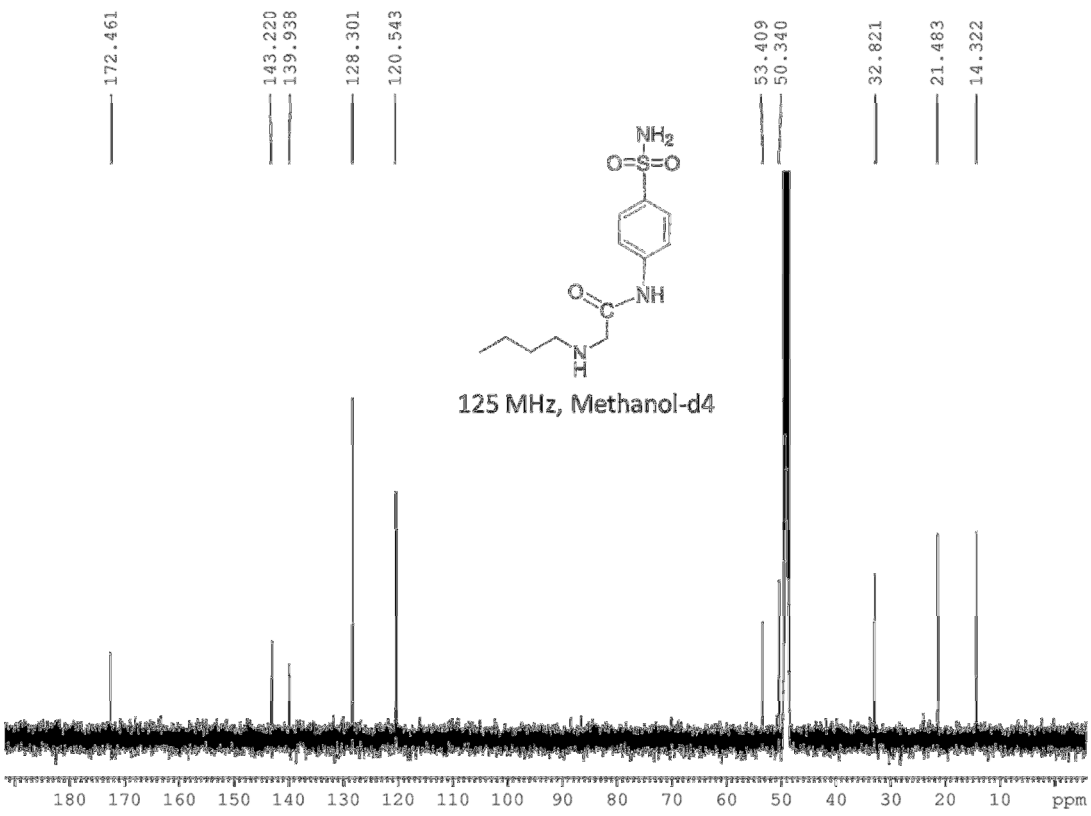
172.461
143.220
139.938
128.301
120.543
53.409
50.340
32.821
21.483
14.322
NH2
O=S=O
NH
O
C
N
H
125 MHz, Methanol-d4
180 170 160 150 140 130 120 110 100 90 80 70 60 50 40 30 20 10 ppm

HIGH RESOLUTION MASS SPECTRA OF COMPOUNDS SYNTHESIZED IN THIS STUDY

Single Mass Analysis
Tolerance = 5.0 PPM / DBE: min = -2.0, max = 80.0
Element prediction: Off
Number of isotope peaks used for i-FIT = 2

Monoisotopic Mass, Even Electron Ions
232 formula(e) evaluated with 2 results within limits (all results (up to 1000) for each mass)
Elements Used:
C: 0-40 H: 0-80 N: 0-4 O: 0-4 S: 0-2

1

29-May-2014
UP_JohnP_1185 19 (1.678)

1: TOF MS ES+
6.41e+003

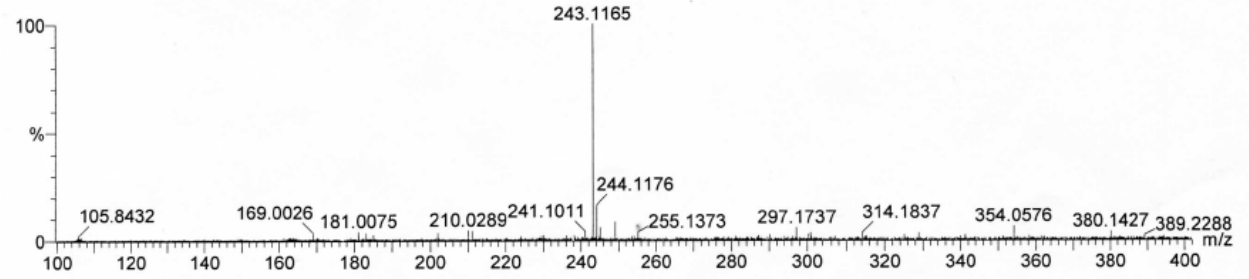

Minimum:				-2.0		
Maximum:		5.0	5.0	80.0		
Mass	Calc. Mass	mDa	PPM	DBE	i-FIT	Formula
243.1165	243.1167	-0.2	-0.8	3.5	9.4	C11 H19 N2 O2 S
	243.1174	-0.9	-3.7	12.5	38.1	C19 H15

2

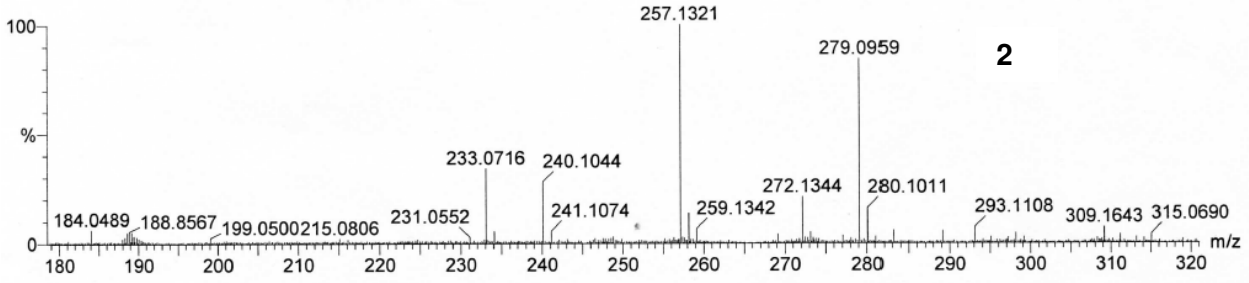

Minimum:				-2.0		
Maximum:		5.0	5.0	80.0		
Mass	Calc. Mass	mDa	PPM	DBE	i-FIT	Formula
257.1321	257.1324	-0.3	-1.2	3.5	21.3	C12 H21 N2 O2 S
	257.1330	-0.9	-3.5	12.5	553.4	C20 H17

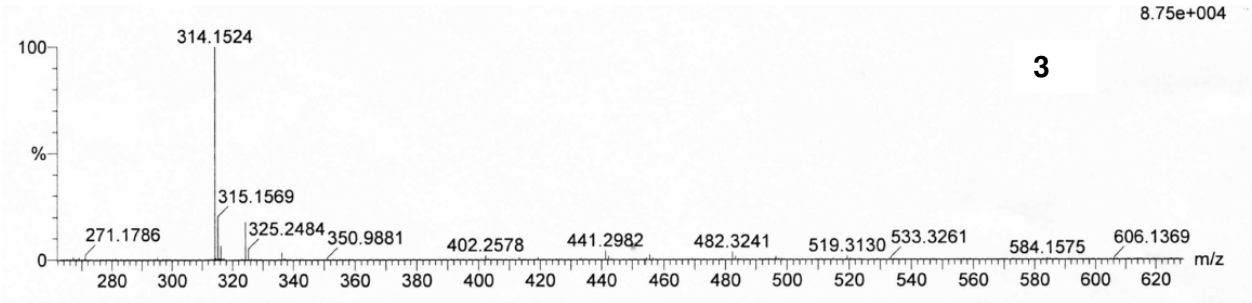

Minimum:						
Maximum:		5.0	5.0	50.0		
Mass	Calc. Mass	mDa	PPM	DBE	i-FIT	Formula
314.1524	314.1538	-1.4	-4.5	4.5	98.6	C14 H24 N3 O3 S

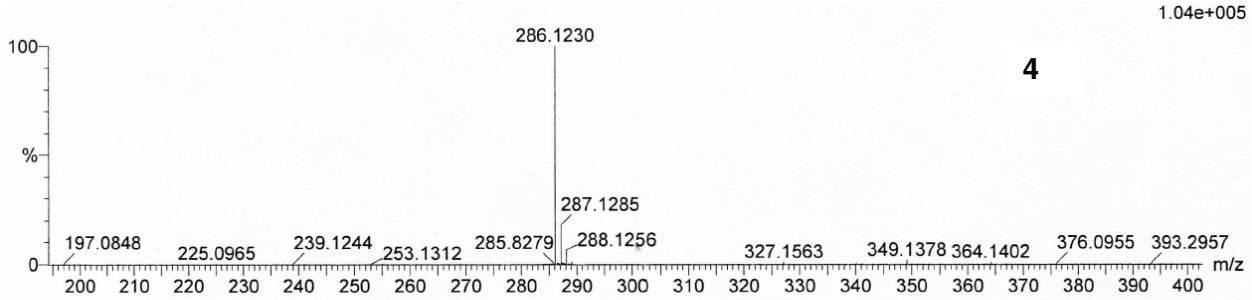

Minimum:						
Maximum:		5.0	4.0	50.0		
Mass	Calc. Mass	mDa	PPM	DBE	i-FIT	Formula
286.1230	286.1225	0.5	1.7	4.5	114.4	C12 H20 N3 O3 S
	286.1232	-0.2	-0.7	13.5	1810.7	C20 H16 N O

REFERENCES

(1) Salvatore, R. N.; Nagle, A. S.; Jung, K. W. *J. Org. Chem.* **2002**, *67*, 674–683.

(2) Addy, P. S.; Saha, B.; Singh, N. D. P.; Das, A. K.; Bush, J. T.; Lejeune, C.; Schofield, C. J.; Basak, A. *Chem. Commun.* **2013**, *49*, 1930–1932.

(3) Ghosh, S.; Isaacs, L. *J. Am. Chem. Soc.* **2010**, *132*, 4445.

(4) Krebs, J. F.; Fierke, C. A. *J. Biol. Chem.* **1993**, *268* (2), 948–954.

(5) Battye, T. G. G.; Kontogiannis, L.; Johnson, O.; Powell, H. R.; Leslie, A. G. W. iMOSFLM. *Acta Crystallogr. Sect. D Biol. Crystallogr.* **2011**, *67* (4), 271–281.

(6) Evans, P. R. *Acta Crystallogr. Sect. D Biol. Crystallogr.* **2011**, *67* (4), 282–292.

(7) Winn, M. D.; Ballard, C. C.; Cowtan, K. D.; Dodson, E. J.; Emsley, P.; Evans, P. R.; Keegan, R. M.; Krissinel, E. B.; Leslie, A. G. W.; McCoy, A.; McNicholas, S. J.; Murshudov, G. N.; Pannu, N. S.; Potterton, E. a.; Powell, H. R.; Read, R. J.; Vagin, A. *Acta Crystallogr. Sect. D Biol. Crystallogr.* **2011**, *67* (4), 235–242.

(8) (a) Adams, P. D.; Afonine, P. V; Bunkóczi, G.; Chen, V. B.; Davis, I. W.; Echols, N.; Headd, J. J.; Hung, L.-W.; Kapral, G. J.; Grosse-Kunstleve, R. W.; McCoy, A. J.; Moriarty, N. W.; Oeffner, R.; Read, R. J.; Richardson, D. C.; Richardson, J. S.; Terwilliger, T. C.; Zwart, P. H. PHENIX. *Acta Crystallogr. Sect. D Biol. Crystallogr.* **2010**, *66* (2), 213–221. (b) McCoy, A. J.; Grosse-Kunstleve, R. W.; Adams, P. D.; Winn, M. D.; Storoni, L. C.; Read, R. J. *J. Appl. Crystallogr.* **2007**, *40* (4), 658–674. (c) Afonine, P. V; Grosse-Kunstleve, R. W.; Echols, N.; Headd, J. J.; Moriarty, N. W.; Mustyakimov, M.; Terwilliger, T. C.; Urzhumtsev, A.; Zwart, P. H.; Adams, P. D. *Acta Crystallogr. Sect. D Biol. Crystallogr.* **2012**, *68* (4), 352–367.

(9) Avvaru, B. S.; Kim, C. U.; Sippel, K. H.; Gruner, S. M.; Agbandje-McKenna, M.; Silverman, D. N.; McKenna, R. A Short. *Biochemistry* **2010**, *49* (2), 249–251.

(10) Emsley, P.; Lohkamp, B.; Scott, W. G.; Cowtan, K. *Acta Crystallogr. Sect. D Biol. Crystallogr.* **2010**, *66* (4), 486–501.

(11) Moriarty, N. W.; Grosse-Kunstleve, R. W.; Adams, P. D. *Acta Crystallogr. Sect. D Biol. Crystallogr.* **2009**, *65* (10), 1074–1080.

(12) Chen, V. B.; Arendall, W. B.; Headd, J. J.; Keedy, D. a.; Immormino, R. M.; Kapral, G. J.; Murray, L. W.; Richardson, J. S.; Richardson, D. C. *Acta Crystallogr. Sect. D Biol. Crystallogr.* **2010**, *66* (1), 12–21.

(13) The PyMOL Molecular Graphics System, Version 1.3 Schrödinger, LLC.

(14) Eisenberg, D.; Schwarz, E.; Komaromy, M.; Wall, R. *J. Mol. Biol.* **1984**, *179* (1), 125–142.